12.3A

Status of Multiple-Sensor Severe Weather Application Development at NSSL

Gregory J. Stumpf[1,2,], Travis M. Smith[1,2], V. Lakshmanan[1,2], Kevin L. Manross[1,2], Kurt Hondl[2]*

[1]Cooperative Institute for Mesoscale Meteorology Studies, University Of Oklahoma, Norman, Oklahoma.
[2]NOAA/National Severe Storms Laboratory, Norman, Oklahoma.

1. Introduction

The National Severe Storms Laboratory (NSSL) has played the primary role in the development and evaluation of U. S. National Weather Service (NWS) severe weather decision-making applications for the Weather Surveillance Radar – 1988 Doppler (WSR-88D). The development process at NSSL begins with basic and applied research including field experiments, theoretical studies, and case studies designed to better understand storms and relate weather to remotely sensed signatures. This research leads to the development of applications, including computer algorithms employing sophisticated image processing and artificial intelligence, and innovative display systems used to enhance the research and development process. Evaluations are conducted using archived case studies as well as real-time proof-of-concept tests at NWS forecast offices (NWSFO) during actual severe weather warning operations. Feedback from the evaluations leads to further research and refinement of applications, and ultimate operational applications for users. The new concepts continue to be tested to determine whether they will be included in future operational systems that help guide and manage the severe weather warning decision-making process.

NSSL developed many of the primary severe weather algorithms for the WSR-88D, and is currently developing improvements to these algorithms. The traditional WSR-88D severe weather algorithms have been designed for use with a single-radar data source. Although NSSL-developed algorithm guidance has led to an improvement of the NWS severe weather warning statistics, it is understood that effective warning decisions can only be made via the integration of information from many sources, including input from multiple remote sensors (multiple radars, mesoscale models, satellite, lightning, etc.). Therefore, it has been a requirement for NSSL to upgrade the traditional single-radar severe weather algorithms to multiple-sensor algorithms to take advantage of additional data source. This reduces the uncertainty of the measurements and increases the accuracy of the detection, diagnosis, and prediction of severe weather. Another requirement of new NSSL algorithms is to rapidly update all input source data so that the latest information is always used. For example, for radar data (both single- and multiple-radar sources), a

"virtual volume" concept is employed which replaces individual elevation scans of data from any radar as they become updated, rather than always processing data at the end of each complete volume scan. Rapidly updating algorithm output will make guidance available for the forecaster earlier, thus leading to an increase in warning lead-time.

NSSL is challenging itself scientifically to provide improved tools and knowledge to improve warning decision making guidance applications. The goals of this endeavor are to 1) improve decision-making efficiency, by providing easy access to the most important information for decision-making (including quick computations for many storms), 2) improve public service with new types of warning products, and 3) improve warning accuracy and lead-time. All these applications must developed in a scientifically sound manner.

The NSSL Warning Decision Support System – Integrated Information (WDSS-II; Lakshman 2002) has provided an invaluable application programmer interface (API) to facilitate the development of many new multiple-sensor severe weather applications for severe weather warning services. In just the past two years (2002-2003), NSSL has developed a variety of new algorithms and major upgrades to existing algorithms. NSSL has converted its suite of single-radar severe weather detection algorithms to operate using multiple radars. These include multiple-radar versions of the Storm Cell Identification and Tracking (SCIT) algorithm (Johnson, et al. 1998), the Hail Detection Algorithm (HDA; Witt et al. 1998). Under development is a multiple-radar replacement for both the Mesocyclone Detection Algorithm (MDA; Stumpf et al. 1998) and the Tornado Detection Algorithm (TDA; Mitchell et al. 1998) known as the Vortex Detection and Diagnosis Algorithm (VDDA). NSSL has also developed a host of new radar diagnostic derivatives, including high-resolution gridded fields of vertically integrated liquid (VIL), Probability of Severe Hail, Maximum Expected Hail Size, Velocity-Derived Rotation, and Velocity-Derived Divergence. Time-integrated gridded fields of some of the above have also been developed, including hail swath information (maximum size and hail damage potential) and velocity-derived rotation tracks. NSSL has also developed new statistical clustering techniques for multiple-scale storm detection and motion estimation, advanced multiple-sensor data quality control using neural networks, and is developing several new multiple sensor prediction algorithms (lightning initiation and prediction and precipitation estimation).

2. Legacy Severe Storms Analysis Program (SSAP)

The original or legacy Severe Storms Analysis Program (SSAP) was the NSSL-developed algorithm system that included some of the severe weather algorithms that are now operational within the National Weather Service (NWS) suite of WSR-88D algorithms. The SSAP components that have been integrated into the WSR-88D include the Storm-Cell Identification and Tracking (SCIT) algorithm, the cell-based Hail Detection Algorithm (HDA), and the Tornado Detection Algorithm (TDA;

sans tracking). One additional component of the SSAP, the Mesocyclone Detection Algorithm (MDA), is presently being engineered for the WSR-88D and will be fully integrated by the summer of 2004. A fifth SSAP component, the Damaging Downburst Prediction and Detection Algorithm (DDPDA; Smith et al. 2002), has yet to be integrated into the WSR-88D system. The version of the TDA in the NSSL SSAP also includes tracking and trend information, which were omitted during WSR-88D integration.

Each of the algorithms, as implemented into the WSR-88D system or within the NSSL SSAP, operates using only single-radar data. In the case of the WSR-88D HDA, some limited thermodynamic information (height of 0ºC and -20ºC levels) from a nearby sounding must be manually input into the algorithm. The NSSL SSAP version of the HDA integrates near-storm environment (NSE) data from the Rapid Update Cycle (RUC) mesoscale model analysis so that the selection of the HDA thermodynamic data is automated and has higher temporal and spatial resolution than synoptic-scale soundings.

Testing of the SSAP was done in offline mode with archived WSR-88D Level II data, or in real-time. Real-time testing was conducted using NSSL's Warning Decision Support System (WDSS; Eilts et al. 1996) at a variety of United States National Weather Service (NWS) Forecast Offices (NWSFO) nationwide since 1993. Both of these legacy systems, the SSAP and the WDSS, were developed as single-radar software systems. All algorithm and radar products were keyed to the individual volume scans and individual radars.

Even with the limitations of single-source algorithms and systems, the WDSS proved valuable for warning improvements. Many of the then-experimental NSSL severe weather algorithms were integrated into the present-day WSR-88D system. This concept continues to be used to test the improvements and additions to the NSSL severe weather analysis applications to be discussed in the following sections.

3. Enhanced Hail Diagnosis Algorithm (EHDA)

NSSL has enhanced the original single-radar cell-based HDA, known as the Enhanced Hail Diagnosis Algorithm (EHDA; Marzban and Witt 2001). This improved hail diagnosis uses a sophisticated and more-accurate Neural Network that integrates the traditional reflectivity radar information with velocity radar information (for rotation and storm-top divergence) as well as NSE data from a mesoscale model. Additional outputs include hail size conditional probabilities for three categories: <4 cm, 4 – 6 cm, and ≥ 6 cm. The output data are made available for icons, tables, and trends. An example of an EHDA table is shown in Fig. 1. NSSL plans to fully integrate the EHDA into the MR-SSAP and as gridded hail products (see next) during 2004.

NSSL Hail Algorithm Output for Volume 275

CELL ID	AZ	RAN	HAIL	SVRH	SIZE	S < 1.5	1.5 - 2.5	S ≥ 2.5	VIL	SHI	MRV	STD	MAX Z	BASE Z
1	253	90	100 %	50 %	2.00	30 %	40 %	30 %	50	208	69	126	58	56
2	241	110	100 %	60 %	1.75	30 %	50 %	20 %	80	255	26	126	58	56
3	343	122	100 %	50 %	1.75	50 %	40 %	10 %	67	210	UNK	UNK	60	60
4	254	94	80 %	20 %	< 1.00	80 %	20 %	0 %	44	69	20	< 40	61	61
5	316	85	90 %	0 %	< 1.00	80 %	20 %	0 %	14	36	22	RF	51	51

Figure 1. Table showing output from NSSL's Enhanced Hail Diagnosis Algorithm (EHDA). Rows represent individual SCIT-detected storm cells, and columns show hail attributes per cell. Selected column headers include POSH (probability of severe hail), MEHS (maximum expected hail size in inches), S<1.5 [probability of hail < 1.5" (4 cm) diameter], 1.5-2.5 [probability of hail between 1.5"-2.5" (4 – 6 cm) diameter], and S≥2.5 [probability of hail ≥ 2.5" (6 cm) diameter].

4. Multiple-Radar SSAP

The Multiple-Radar Severe Storms Analysis Program (MR-SSAP; Stumpf *et al.* 2002) extends the concepts of the legacy SSAP into the multiple-radar, multiple-sensor realm. The present architecture of each algorithm is to detect two-dimensional (2D) features on radar elevation scans. At the end of each complete radar volume scan, the 2D features are vertically associated to create 3D detection products (e.g., storm cells, mesocyclones, TVSs). These 3D detections are also time-associated with 3D detections from a previous volume scan to produce tracks and trends. This method leads to a variety of disadvantages. First, algorithm products are only generated at the end of a volume scan, which is typically 5-6 minutes after the first elevation scan of the volume scan is collected. This has led to warning meteorologists placing less weight on the algorithm products for warning guidance and more weight on analysis of the more-timely radar data alone without the additional guidance. Second, storm and tornado evolution can typically be very rapid, and 5- or 6-minute algorithm update rates may be inadequate. Third, storms can be poorly sampled at very near ranges to the radar (cone-of-silence) and at far ranges (radar horizon, lower sampling resolution).

An early attempt at a multiple-radar SSAP compared the algorithm detections from the various single-radar sources and determined the "best" radar to use as the one sensing the storm or mesocyclone/TVS with the strongest intensity. This method, called the "County Warning Area (CWA) Table", did not take advantage of combined information from multiple radars, and thus issues like poor sampling still plagued the system. It also did not synchronize for the time difference between the multiple radar scans through similar features.

The MR-SSAP instead *combines* the two-dimensional information from multiple radars and uses these data sets to produce 3D detections. This will allow for a more complete vertical sampling of storms and mesocyclones/TVSs where vertical sampling resolution is degraded. Signatures are now better sampled where adjacent radars are adding data to poorly sampled regions such as cones-of-silence (Fig. 2). Multiple radar data are mosaicked into "virtual volume" scans (Lynn and Lakshman, 2002), with the

latest elevation scan of data replacing the one from a previous volume scan. This method gives a complete volume scan at any point in time. Vertical and time association is then performed at regular intervals with the last several minutes of 2D features within a "virtual volume" enabling rapid updating of algorithm output and time-synchronization of the multiple-radar data. Output products can be generated as soon as a new radar elevation scan is included in the virtual volume (10-20 seconds). Presently, the NSSL system runs the updates at 60-second intervals for better warning management. The rapidly updating virtual volume can also run with single radar mode if coverage and outages dictate. The virtual volumes are designed to be VCP-independent, and can be integrated with other "gap-filling" radar platforms, including FAA (e.g., TDWR) and commercial radars. Products are keyed to a four-dimensional earth-relative coordinate system (latitude, longitude, height above MSL, time).

5. Multiple-Radar SCIT and HDA

Reflectivity information from multiple radars is used to detect and diagnose storm cells. Virtual volumes of radar data containing the latest information from each radar for the previous 5 minutes are combined to produce vertical cores representing storm cells. The vertical association technique clusters 2D features from each of the radars within the 5 minute-window into 3D storm features (Fig. 3). Time-to-space conversion is used to account for storm motion for the older 2D features. 2D feature components can be drifted in time and space using a number of different advection options, including input or mean wind from mesoscale model data, actual motion of mature storm features, or a combination of both. The vertical association technique is repeated every 60 seconds using all 2D features that are less than 5 minutes old. The multi-radar reflectivity data from the 2D features used to construct the 3D storm cell detections are diagnosed to give traditional cell-based attributes such as vertically integrated liquid (VIL). Cell-based HDA information (POSH, hail size) is also diagnosed using the combined multiple radar data, as well as thermodynamic data from mesoscale models (Fig. 4). The cell-based storm and hail diagnoses are executed rapidly at 1-minute intervals. Storm cells are also tracked in time (60-second intervals), attribute data are available for 60-second interval trend information, and 30-minute forecast positions are made (Fig. 5).

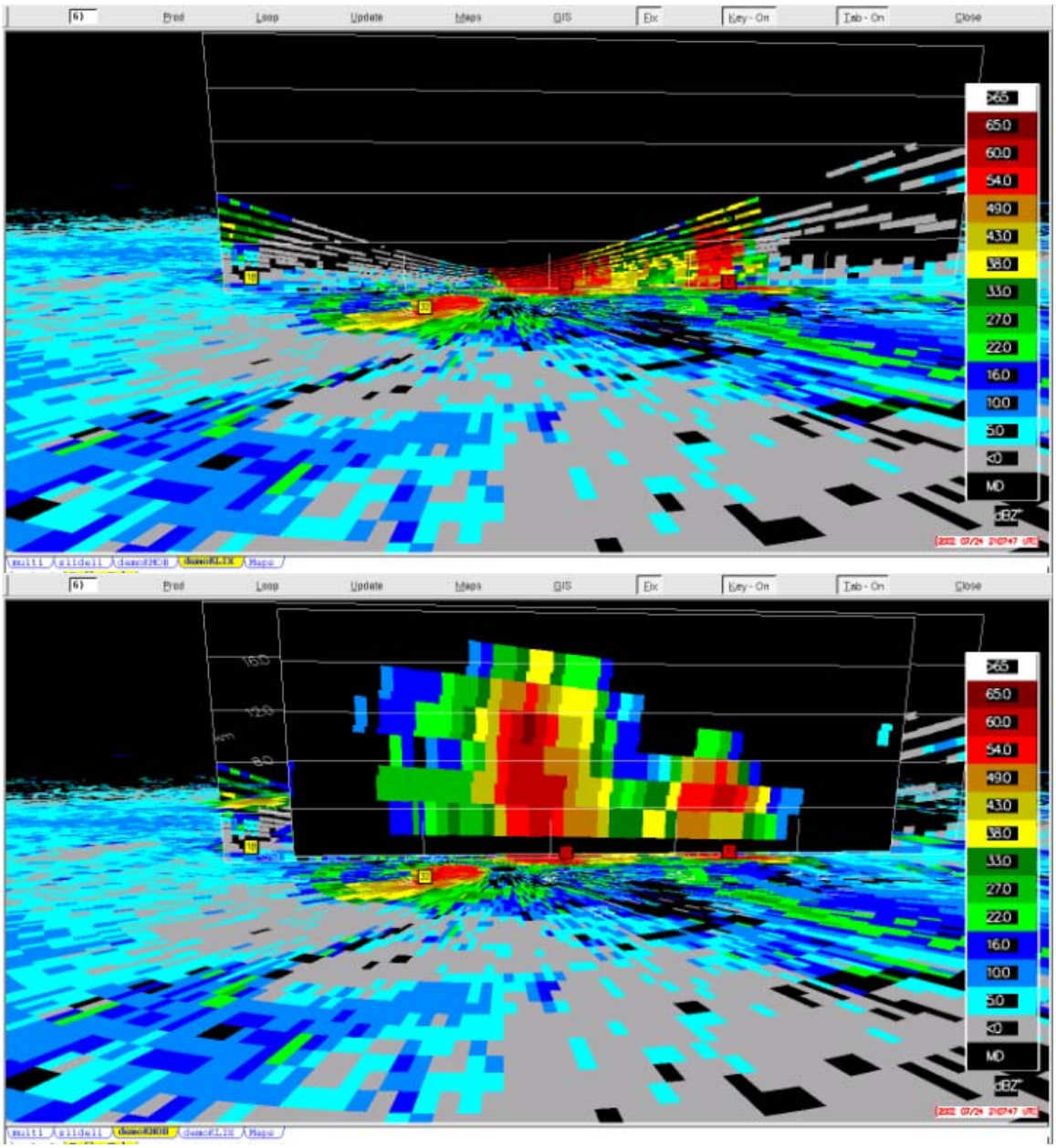

Figure 2. WDSSII image of WSR-88D Slidell, Louisiana, reflectivity data with horizontal and vertical planes as viewed in a three-dimensional "airplane viewpoint" from south of the storm (top). WSR-88D Slidell, Louisiana, horizontal and WSR-88D Mobile, Alabama, vertical reflectivity planes of same data from same 3D viewpoint (bottom). Note that data from Mobile radar are used to fill the Slidell data-void cone-of-silence region. Multiple Radar-SCIT icons are represented by numbered red or yellow squares overlaid on radar data.

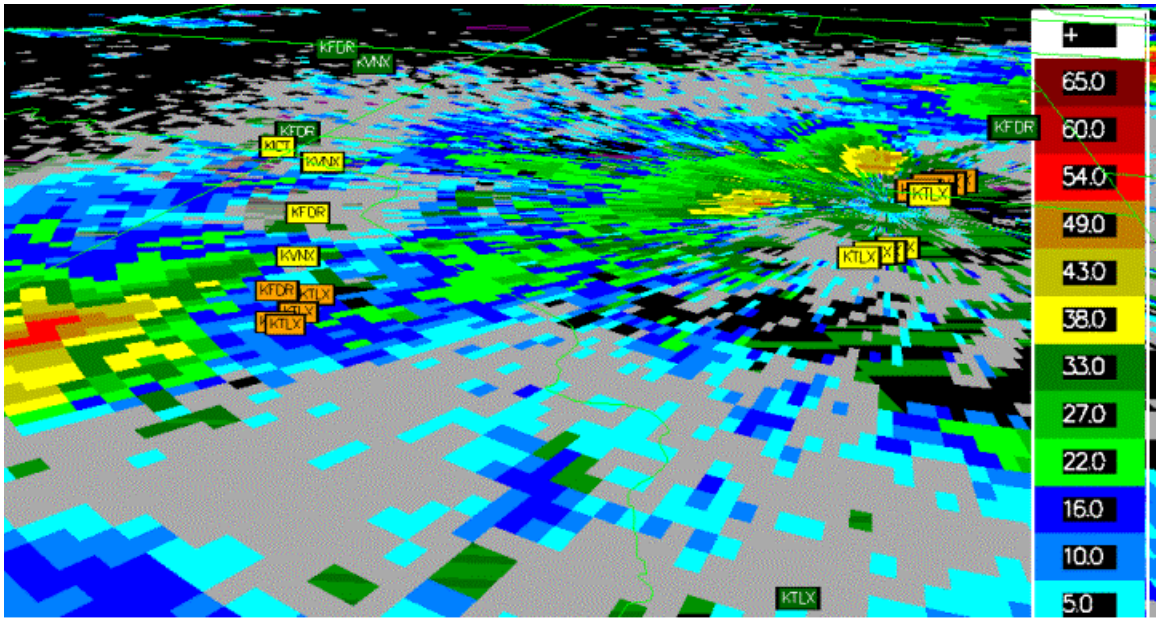

Figure 3. WDSSII image of WSR-88D Oklahoma City, Oklahoma, 0.5° reflectivity data as viewed from an "airplane" angle from the south of the radar, looking down and northwest. Radar location is in the upper right of the image. Overlaid are centroid locations of Multiple Radar-SCIT 2D features, with the 4-letter radar identifier from the originating radar indicated. Icons are color-coded by maximum reflectivity. Note clustering of 2D features to the southwest of the radar. This represents a Multiple Radar-SCIT storm cell comprised of 2D features from multiple radars.

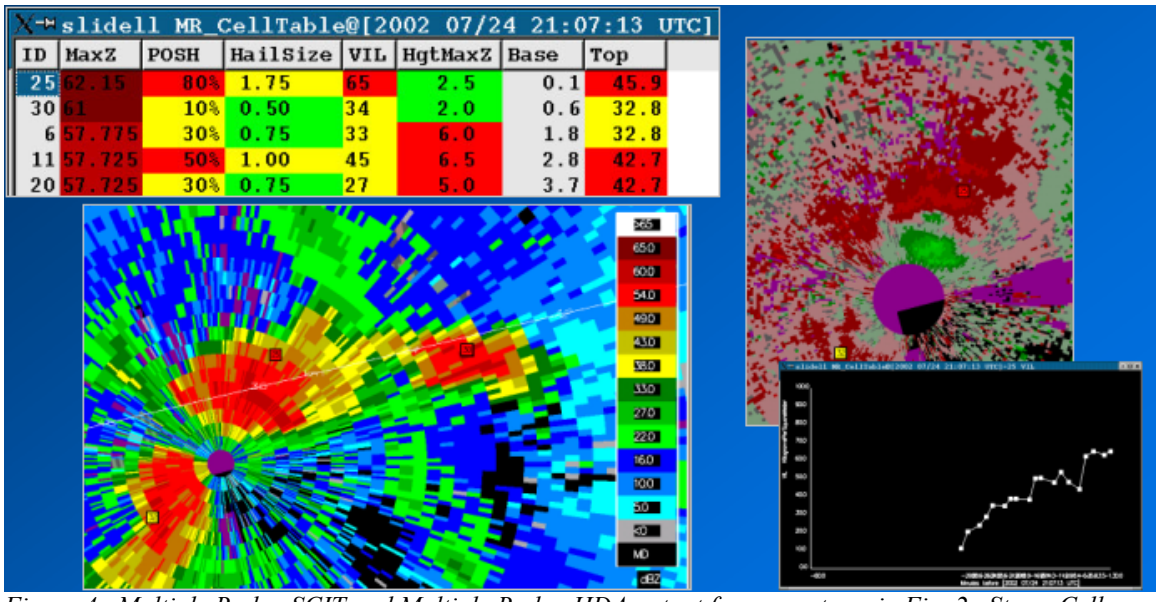

Figure 4. Multiple Radar-SCIT and Multiple Radar-HDA output for same storm in Fig. 2. Storm Cells are represented by numbered red or yellow squares overlaid on radar data (lower left and upper right). Storm cell and hail diagnostic information is presented in the table in the upper left. 60-second rapidly updating trend of Multiple Radar-SCIT cell-based VIL is shown at the lower right.

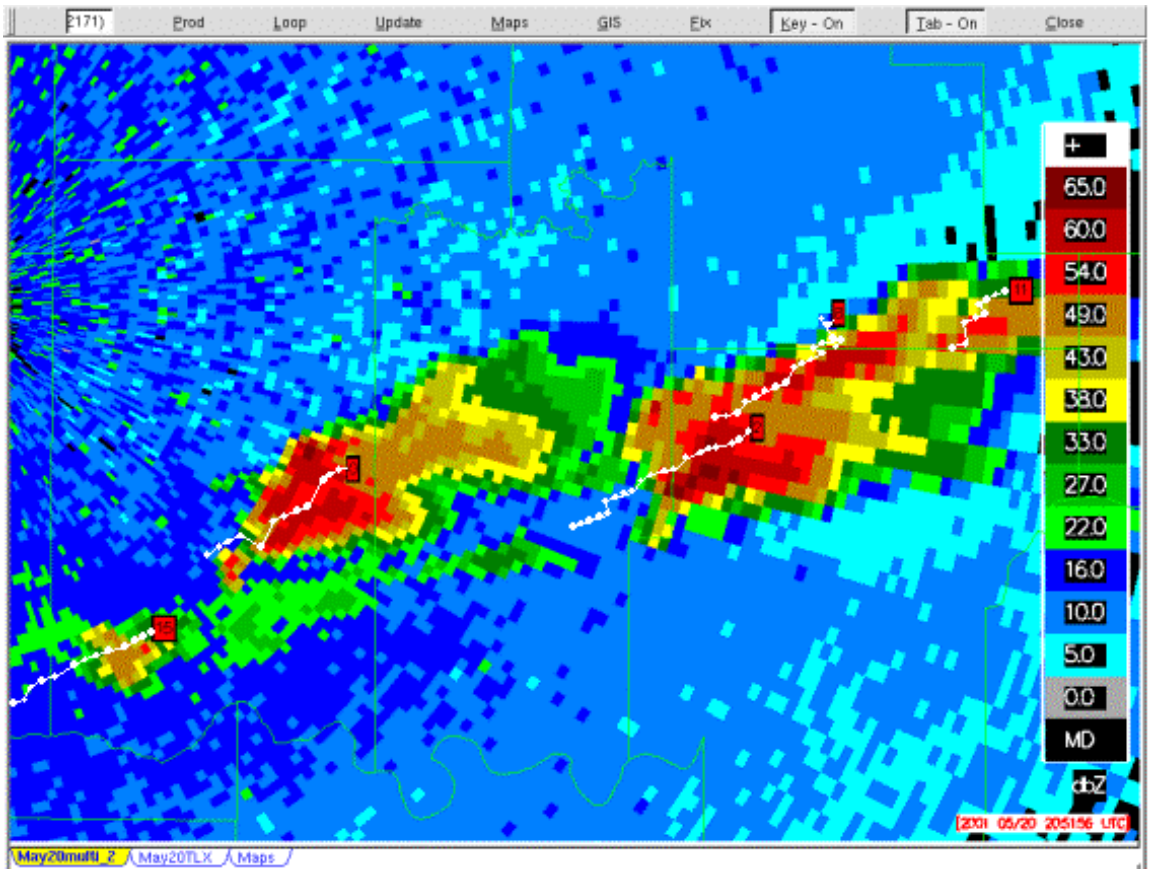

Figure 5. Oklahoma City, Oklahoma, WSR-88D data and current Multiple Radar-SCIT storm locations (red numbered square icons) and 60-second past positions (white dots and lines). Note that current storm locations are already downstream of latest reflectivity data from Oklahoma City WSR-88D, owing to new information from Tulsa, Oklahoma, and Fort Smith, Arkansas, WSR-88D data (not shown).

6. Four-Dimensional Multiple-Radar Applications

NSSL has developed the capability to merge multiple-radar data into four-dimensional (4D) grids (Zhang et al., 2001, 2003). These grids are specified in latitude/longitude/height/time coordinate systems. Values in grid cells sensed by more than one radar are combined using a time and an inverse-distance weighting scheme. Terrain information is combined with beam power-density cross-sections to determine the amount of beam blockage. The data can be continuously updated each time an elevation scan from one of the radars is updated (every 10-20 seconds). Older radar data in the grid can also be advected using the NSSL motion estimation algorithm (see later). Given ample computational resources, it is possible to create 4D radar grids to cover a very large region, including the Continental U.S. It is also possible to combine radars from different networks (WSR-88D, TDWR, commercial radars) into multiple-radar grids.

Presently, WSR-88D gridded maps of maximum vertical reflectivity (sometimes known as "Composite Reflectivity") and Vertically-Integrated Liquid (VIL) are presented with poor

spatial (2 km Cartesian grids) and poor temporal (5-min updates) resolution (Fig. 6). Using the rapidly updating 4D multiple-radar grids, NSSL has developed high-resolution spatial (1x1 km) and temporal (using virtual volumes with 10-20 second updates) versions of these popular products (Fig.7). Other products include reflectivity at constant heights ("CAPPIs"), maximum reflectivity within any layer specified by two constant height levels, height of maximum reflectivity, maximum heights of constant reflectivity values (e.g., "Echo Tops"), and VIL Density (VIL divided by the depth of integration). The faster updates provided by the virtual volumes allows for more rapid access to the diagnostic fields, versus access only once per single radar volume scan and at the end of those volume scans.

Having radar data on a lat/lon/height grid makes it easier to combine with data from other sensors, particularly environmental data from a mesoscale model (e.g., 20 km RUC). The input of thermodynamic data is useful for deriving values of reflectivity at constant temperature levels (e.g., at the melting level of 0ºC) and temperature layers, the height of constant reflectivity values above certain temperature levels (e.g., height of 50 dB*Z* level above the 0ºC level), and the various hail diagnosis parameters described in the next section.

The process by which reflectivity data from multiple radars is merged can also be used to combine other multiple radar fields, such as fields of scalar velocity derivatives from single radars (e.g., azimuthal and radial shear – see later section).

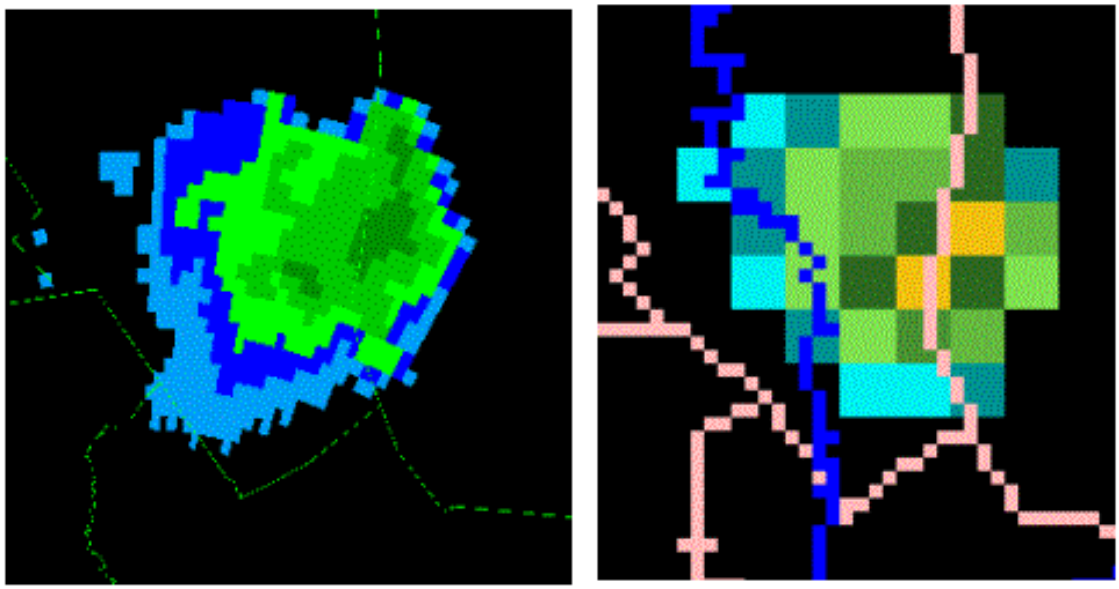

Figure 6. High-resolution polar gridded Vertically Integrated Liquid (VIL) on left (1km by 1º, and low-resolution Cartesian gridded WSR-88D VIL on right (2km by 2km).

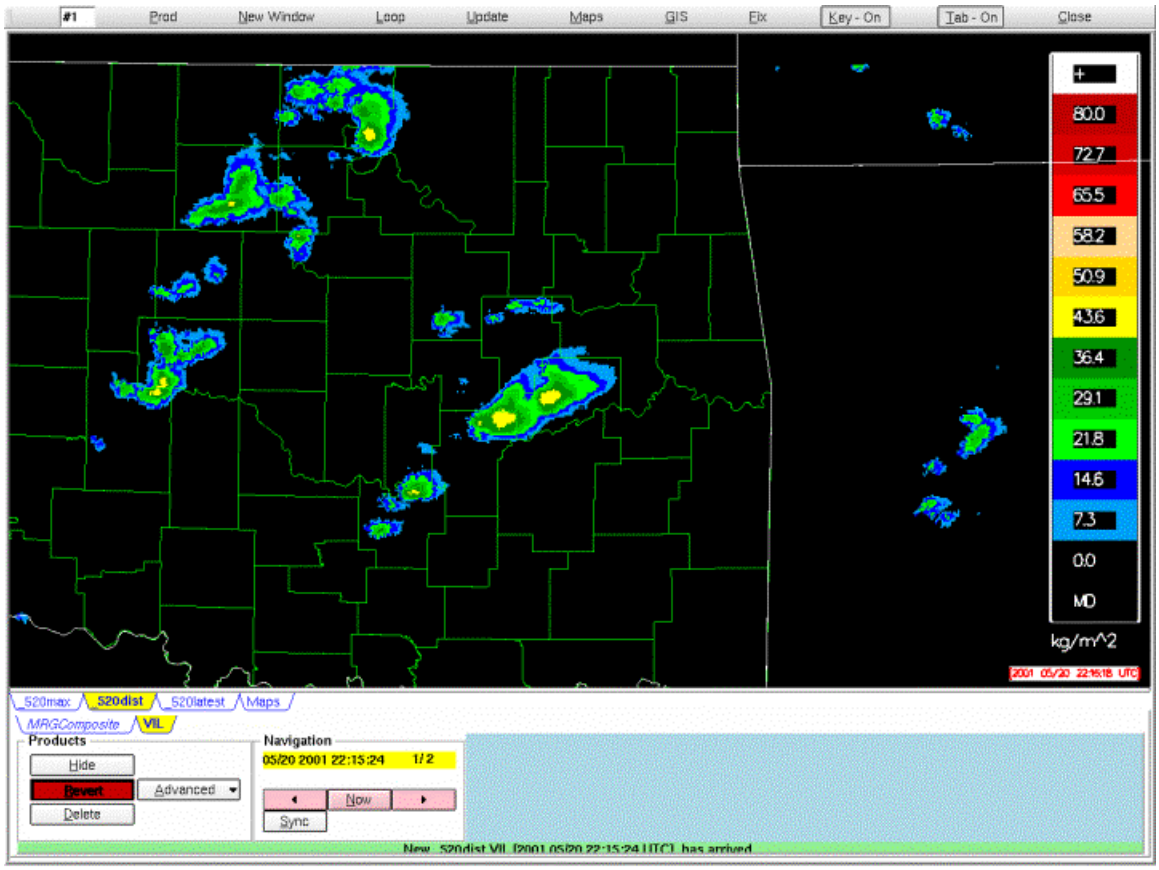

Figure 7. Multiple-radar high-resolution gridded Vertically Integrated Liquid (VIL) (roughly 1 by 1 km). Data from three radars supplied the grid.

7. Gridded Hail and Hail Swath Diagnostic Products

The techniques used to derive popular WSR-88D cell-based hail products from the HDA have been incorporated into high-resolution gridded products similar to the high-resolution VIL product. Using the Severe Hail Index (SHI; Witt et al. 1998), a product similar in concept to VIL, but with contributions of higher reflectivities above freezing levels included, probability of severe hail and maximum expected hail size products are derived.

This is a different paradigm in hail information delivery than is commonly used within national U.S. warnings. Geo-spatial information on hail probability and hail size can be made available (versus single values per storm cell), which allows a user to diagnose which portions of storms contain large hail. Geo-spatial information also has the added benefit of improving hail warning verification, since the locations of the largest hail can be estimated. The gridded hail size data can also be accumulated over time to provide precise hail swath maps, showing both maximum hail size by location, and hail damage potential (combination of hail size and duration of hail) (Fig. 8). High spatial and temporal resolution grids can be extracted from both single radar data as well as multiple-radar mosaics. The multiple radar grids have a spatial

resolution (of roughly 1x1 km^2, and high temporal resolution using virtual volumes with 10-20 second updates (Fig.9). Thermodynamic data is integrated from mesoscale numerical models, which also offers better temporal and spatial resolution than 12 hourly rawinsonde updates. Future work is planned to adapt the Enhanced-HDA to a geo-spatial grid, integrating reflectivity, velocity-derived products (see next section), and environmental thermodynamic and kinematic information from mesoscale models.

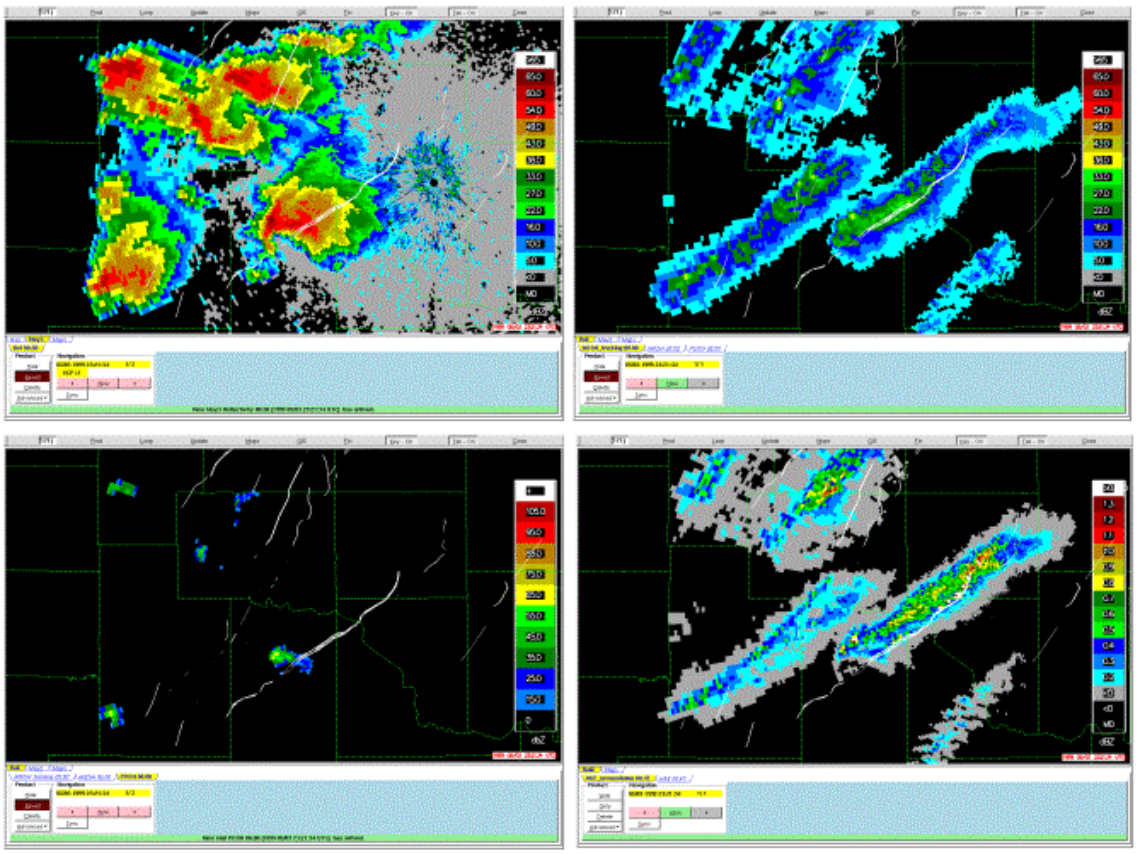

Figure 8. Oklahoma City, Oklahoma, WSR-88D reflectivity during 3 May 1999 tornado outbreak (upper left); High-resolution Gridded Probability of Severe Hail (POSH) field (lower left); Hail size swath field (upper right), Hail Damage Potential Accumulation field (lower right). Overlaid thin white lines are the actual tornado track locations obtained from NWS damage survey.

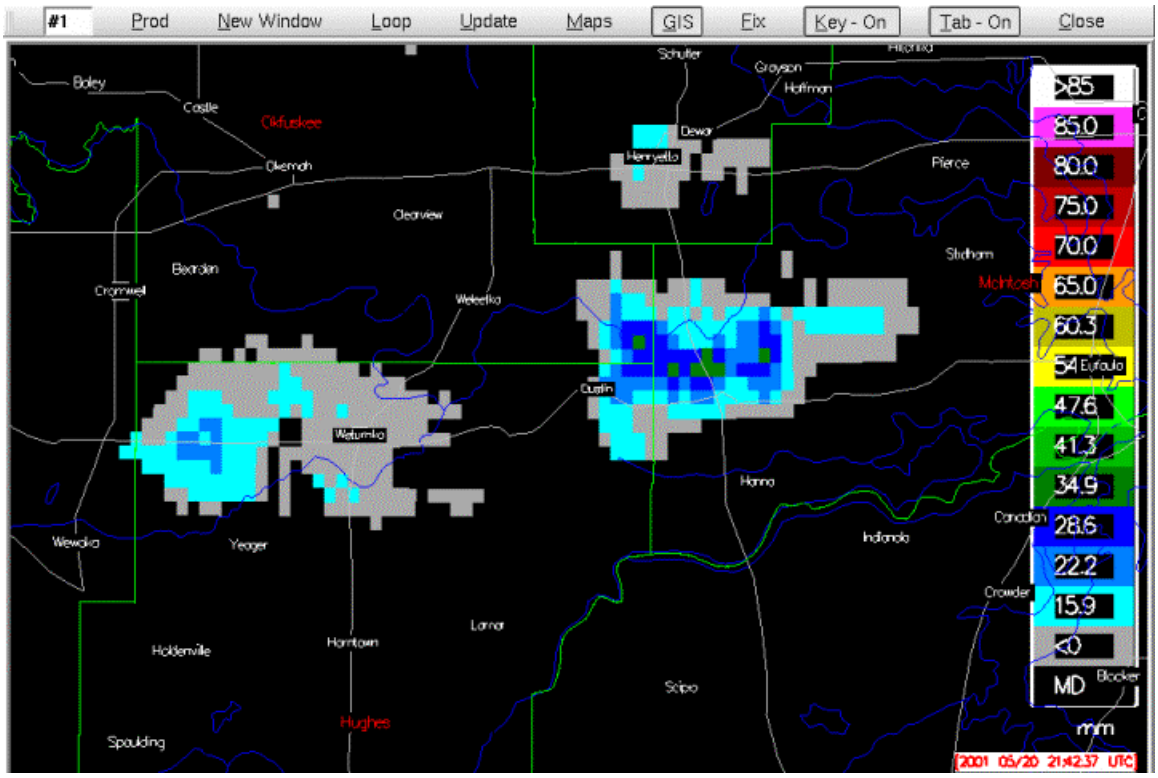

Figure 9. Multiple-radar high-resolution gridded Maximum Expected Hail Size (MESH)(roughly 1 by 1 km). Data from three radars supplied the grid.

8. Storm-Scale Vortex Detection and Diagnosis

More sophisticated techniques are being developed to accurately detect and diagnose storm-scale rotation in radar velocity data. Present techniques (TDA, MDA) search for patterns of vertically correlated azimuthal shear in single-Doppler velocity data (Mitchell et al. 1998; Stumpf et al. 1998). Current research has shown that these azimuthal shear techniques are worse at estimating vortex location, size, and strength than techniques that employ velocity derivatives of rotation and divergence. Traditional azimuthal shear techniques can also produce false detections along non-rotation signatures. Radial velocity values are a factor of single-radar viewing angles (one component of velocity is measured – that along the radar beam). Also, the traditional algorithms are heuristic (use pre-defined thresholds and rule bases) and are centroid based, which can lead to much instability when combining data across elevation and volume scans (in the vertical and across time).

Using a Linear Least Squares Derivative (LLSD) technique described by Elmore et al. (1994) and adapted by Smith et al. (2003), derivatives for azimuthal shear and divergence are produced in gridded form. These scalar velocity derivatives are much less dependent on radar viewing angle, which allows for the combination of gridded shear derivative fields from multiple radars. Gridded azimuthal shear derivative fields from single and multiple radars can also be accumulated over time and within specific height layers (e.g., 0-4 km

AGL), providing a proxy for "rotation tracks" of mesocyclone features (Fig. 10). The information in these "rotation tracks" is simply a diagnostic of the velocity data, and does not suffer from the instabilities inherent to heuristic and centroid-based methods. Within one "rotation track" image is information about the past track of the events (which can be used to nowcast the future position) as well as the trend of the strength of the rotation in those events. Also, the rotation track product can serve as a very valuable verification tool to help determine where unreported or unobserved tornadoes may have occurred. One image such as Figure 10 can replace the time-consuming process of replaying radar data and manually tracking individual mesocyclones, and can be used to help deploy damage survey teams.

Both the LLSD azimuthal shear and divergence fields can be combined to compute a true rotation field. Combining LLSD rotation fields from multiple radars and three-dimensionally in the vertical can be used to depict the vertical "tube" of the mesocyclones (Fig. 11). These 3D rotation fields will be used as the basis for a new Vortex Detection and Diagnosis Algorithm (VDDA) to replace the MDA and TDA.

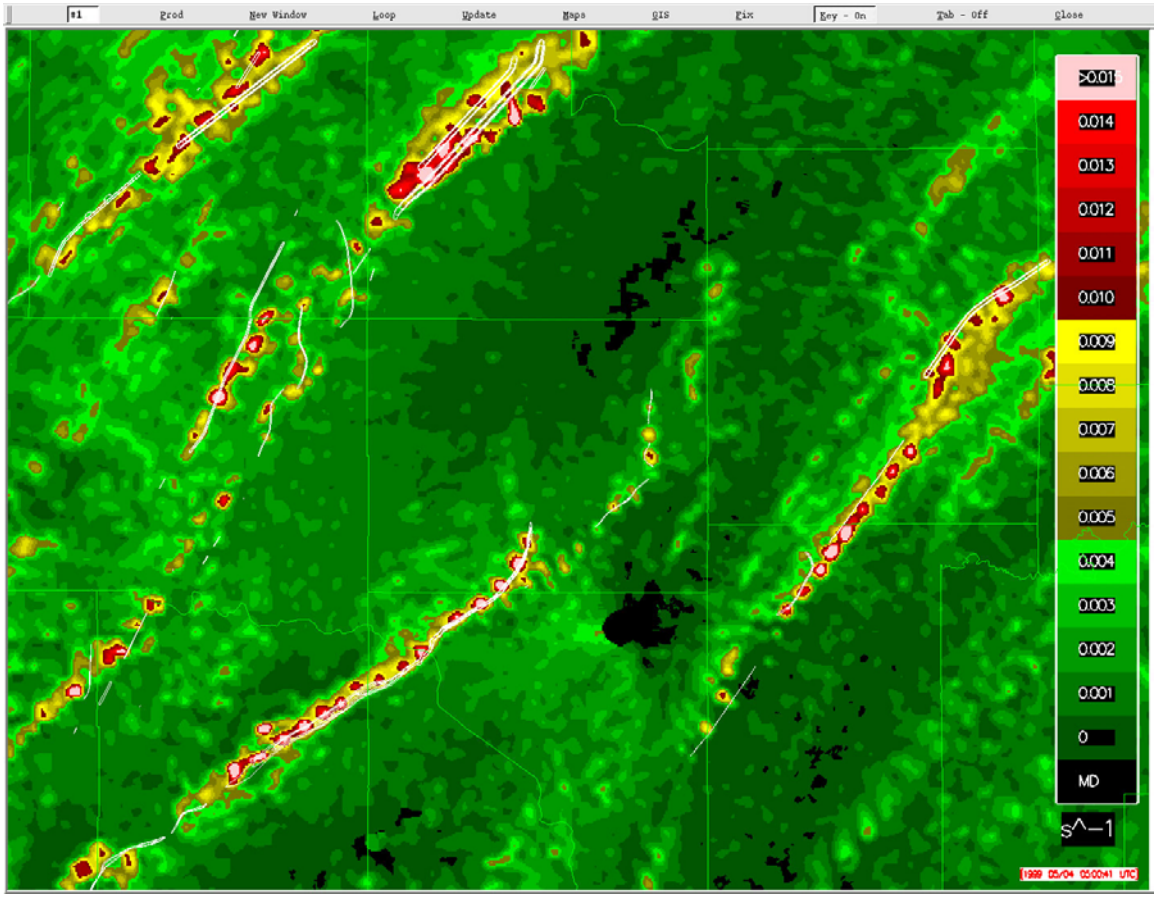

Figure 10. Six-hour gridded accumulated LLSD azimuthal shear derivative field for the 3 May 1999 tornado outbreak in Central Oklahoma. Overlaid thin white lines are the actual tornado track locations obtained from NWS damage survey.

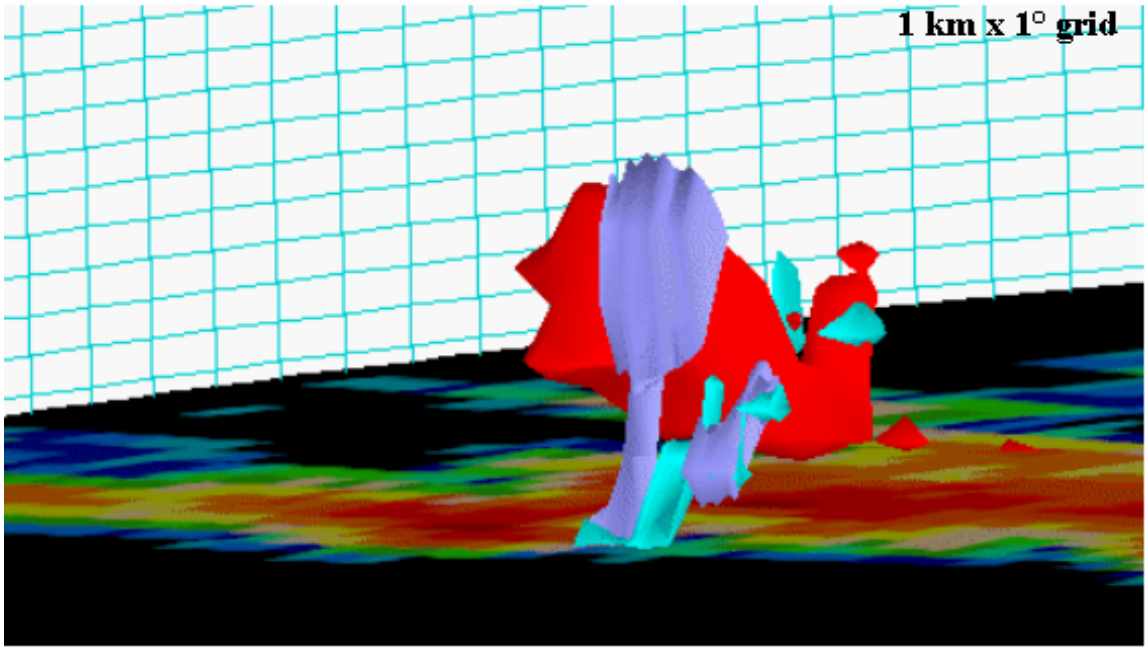

Figure 11. Three-dimensional image of an isosurface of rotation in a supercell storm (lavender represents vertical vorticity exceeding 10^{-2} s^{-1}).

9. Motion Estimation

NSSL is currently developing a sophisticated technique to forecast the motion, growth, and decay of two-dimensional storm fields (Lakshmanan 2003). This is not a cell tracker, but rather a forecast of 2D radar or satellite fields. Present cell-tracking algorithms (e.g., SCIT) rely on heuristic rule bases and centroid tracking schemes, which can cause a number of tacking instabilities. The motion estimation application begins with a statistical clustering technique that can segregate multiple scales of reflectivity features, which are hierarchical in nature (larger clusters contain smaller clusters, and so on). These clusters are tracked independently with greater stability than the centroid based algorithms. The product also contains a storm growth and decay component. Time histories of tracked cluster can then be diagnosed for trend information.

Up to 60-minute forecasts of these two-dimensional products can be produced (Fig. 12). The technique also produces a high-resolution motion field that can be used to advect any two-dimensional product, such as precipitation accumulation, VIL, hail, rotation, or lightning fields to provide up to 60-minute forecasts of these phenomena. The high-resolution motion estimates are also used within the 4D multiple-radar grids to advect the slightly older data (up to 10 minutes old) forward in time. Coupled with the virtual volume rapid updating, this has the added benefit of removing the "strobing" effect commonly observed in precipitation accumulation maps due to the discrete volume scan sampling intervals (every 5 or 6 minutes).

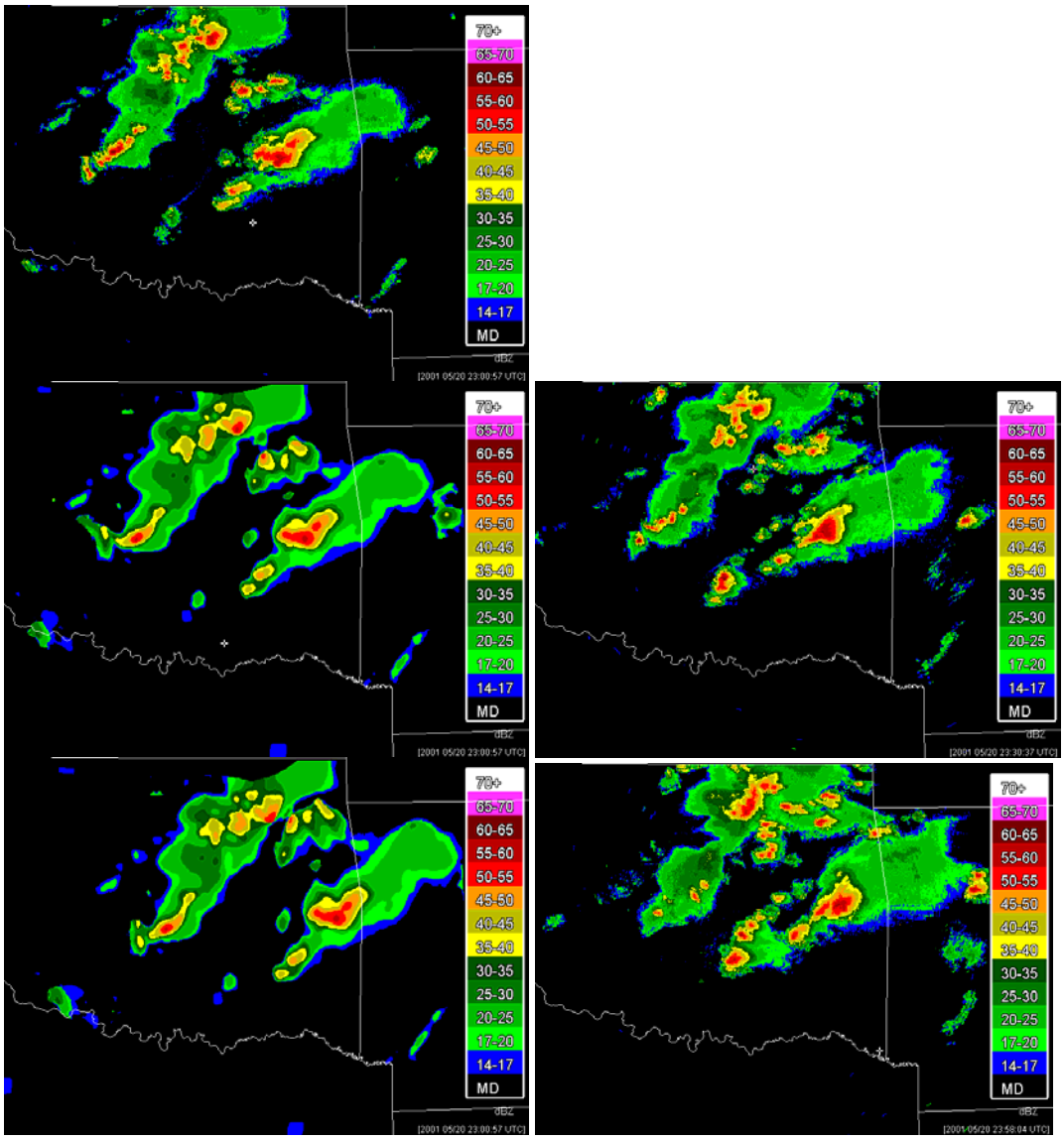

Figure 12. Reflectivity forecasts from the WDSS-II Motion Estimation algorithm, and verification using actual data. Current reflectivity field (top left), 30 minute forecast (middle left), 30 minute verification (middle right), 60 minute forecast (bottom left), and 60 minute verification (bottom right).

10. Quality Control Neural Network (QCNN)

Radar reflectivity fields are comprised of meteorological echo and data artifacts such as ground clutter, anomalous propagation (AP), and chaff. Most severe weather applications depend on pristine data to properly detect and diagnose phenomenon, so these artifacts need to be identified and removed prior to processing. Also, many applications require that other meteorological returns not associated with precipitation (e.g., clear air blooms) be removed.

NSSL has developed a Quality Control Neural Network (QCNN; Lakshmanan et al. 2003) designed to look at properties of the three moments of radar data (reflectivity, radial velocity, spectrum width) as well as multi-sensor "cloud

cover" data (combined IR satellite and surface temperatures) to segregate precipitation from non-precipitation (and data artifact) echo. This is used as a preprocessor to certain severe weather applications, such as mesocyclone and TVS detection and quantitative precipitation estimation. The QCNN has been shown to improve upon current techniques such as the Radar Echo Classifier (REC; Kessinger et al. 2003). Shown below is an example of a reflectivity field before (Fig 13a) and after removal (Fig 13b) of non-precipitation echo with overlaid mesocyclone detection centroids. The velocity dealiasing process is frequently problematic in areas of clear air bloom or AP, and this can lead false detections of mesocyclones. This is commonly observed when diagnosing mesocyclone climatologies over long-term testing (which mostly includes periods without precipitation). By segregating the precipitation areas, the false mesocyclone detections are removed (Fig 13b) without impacting the true detections within precipitation areas.

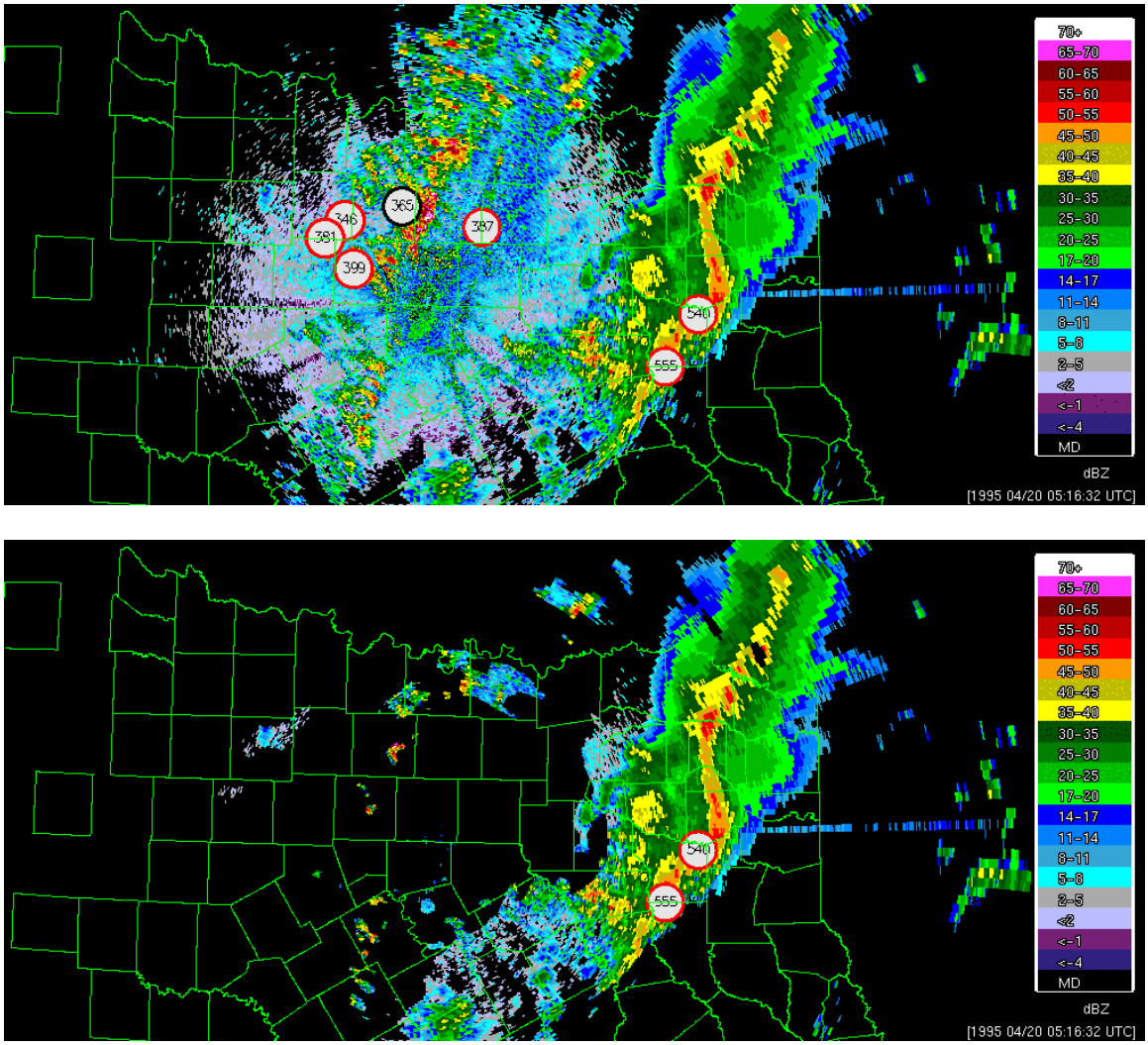

Figure 13. a) (top) Original reflectivity field of a squall line case with clear air, AP, and clutter returns near the radar. Overlaid circles are mesocyclone detections. B) (bottom) Reflectivity field and overlaid mesocyclone detections after QCNN removed non-precipitation echo. Data are from KFWS (Fort Worth TX) 20 Apr 1995 05:36 UTC.

11. Near-Storm Environment (NSE) Algorithm

NSSL has developed an algorithm that analyzes mesoscale numerical model output and derives a large number of sounding parameters. These derived gridded data are used as source input to a number of our current and proposed algorithms. The model initial analysis fields are used to provide greater temporal and spatial resolution of important environmental data for the multiple-sensor applications. For example, rapidly updating thermodynamic data (heights of 0C and –20C levels) are input into the cell-based and grid-based hail diagnosis algorithms. The rapidly updating information can be used to capture rapidly evolving thermodynamic fields or fields with large spatial gradients much better than rawinsonde information.

12. R&D Application Development Environment using WDSSII

The Warning Decision Support System - Integrated Information (WDSS-II; Hondl 2002, Lakshman 2002) greatly facilitated the research and development process of these new applications. The WDSS-II is the result of over 10 years of research, application development, and operational testing at NSSL and NWS forecast offices. WDSS-II is a capable real-time data ingest and processing system that can be used to evaluate experimental applications in an operational setting. It is also a powerful application development tool. It is easy to add new products and concepts, and it provides a seamless path from data ingest, data processing, and output using standard formats. This should improve the pace of science and technology infusion into operational warning decision systems.

The WDSS-II components include 1) data ingest of data from multiple radars and sensors (in archive mode or in real-time), 2) detection, diagnosis, and prediction multi-sensor algorithms, 3) an interactive display designed specifically to effectively manage and provide rapid access to the most important information for decision-making (including novel 4D earth-relative base-data visualization techniques), and 4) an infrastructure to support application development, data ingest and distribution, configuration, and extensible output data formats.

The WDSSII has been developed using economical Linux systems and uses an object-oriented design with a library of functions and classes for real-time (or archived) multiple-source data input, manipulation, and output. The WDSSII integrates data from a variety of sources (multiple radars, satellites, mesoscale models, lightning) and converts all the data to a common coordinate system (3D earth-relative and time-synchronized). The object-oriented structure of the code also facilitates the development of functions that can be reused using other data sources (such as other radars besides WSR-88D, including FAA and commercial “gap-filling” radars). The computing structure is distributed, and can be threaded across multiple processors depending on the amount of data and number of applications. The system uses standard output formats (NetCDF for gridded data; XML for graphics, tables, and trends; shapefiles for geo-located graphics) for use in a variety of display technologies (e.g., AWIPS, OpenGL, Java, Web-based), where output data can be customized on

the fly. Application development is facilitated by the use of contemporary software development tools [e.g., Concurrent Versions System (CVS) software repository; auto-generated Doxygen object class documentation].

13. Conclusion and Future Work

The pace of this innovative development would not have been possible without WDSSII as an effective research and development tool and testing platform. Many of the ideas for these applications were considered many years prior to the development of the WDSSII, and are now coming to fruition at NSSL. There are many more concepts that have yet to be implemented, including some suggestions made by NWSFO forecasters after exposure to the applications in actual warning operations. This represents a quantum leap in the improvement of warning and situational awareness technology.

These new multiple-sensor applications represent only the first phase of improvements for the NSSL experimental severe weather applications. NSSL plans to expand the use of input from other sensors into the algorithms (including mesoscale model, lightning, surface, and satellite data) for a full three-dimensional multiple-sensor suite of severe weather applications. An upgrade to our application and display systems will continue to be tested during 2004 at several U.S. NWSFO and international testbeds. The results of these tests will lead toward eventual improvement of the severe weather applications for warning services and systems nationally and worldwide.

ACKNOWLEDGMENTS

Thanks go to the NSSL WDSS-II development team of Don Bailor, Lulin Song, Jianting Zhang, Kevin Manross, and Claire Thomas. Don Burgess and Kim Elmore provided scientific guidance for this work. Mark Benner, Karen Cooper, and Robert Toomey provided the hardware and data ingest support and technical assistance for the real-time NWS forecast office tests. Rodger Brown and several anonymous reviewers provided comments on the manuscript. This work has been primarily funded via sources from the Federal Aviation Administration, the NEXRAD Radar Operations Center, the National Science Foundation, the National Severe Storms Laboratory, and under NOAA-OU Cooperative Agreement #NA17RJ1227.

REFERENCES

Eilts, M. D., J. T. Johnson, E. D. Mitchell, S. Sanger, G. J. Stumpf, A. Witt, K. W. Thomas, K. D. Hondl, D. Rhue, and M. Jain, 1996: Severe weather warning decision support system. *Preprints, 18th Conf. on Severe Local Storms*, San Francisco, CA, Amer. Meteor. Soc., 536-540.

Elmore, K.M, E.D. Albo, R.K. Goodrich, and D.J. Peters, 1994: NASA/NCAR airborne and ground-based wind shear studies. Final Report, contract no. NCC1-155, 343 pp.

Hondl, Kurt, 2002: Current and planned activities for the Warning Decision Support System – Integrated Information (WDSS-II). *Preprints, 21st Conference on Severe Local Storms*, San Antonio, TX, Amer. Meteor. Soc., 146-148.

Johnson, J. T., P. L. MacKeen, A. Witt, E. D. Mitchell, G. J. Stumpf, M. D. Eilts, and K. W. Thomas, 1998: The Storm Cell Identification and Tracking (SCIT) algorithm: An enhanced WSR-88D algorithm. *Wea. Forecasting*, **13**, 263-276.

Kessinger, C., S. Ellis, and J. Van Andel, 2003: The radar echo classifier: A fuzzy logic algorithm for the WSR-88D. *Preprints, 19th International Conf. on Interactive Information and Processing Systems (IIPS) for Meteor., Oceanography, and Hydrology,* Amer. Meteo. Soc., Long Beach, CA, (CD Preprint).

Lakshmanan, V., 2002: WDSSII: an extensible, multi-source meteorological algorithm development interface. *Preprints, 21st Conf. on Severe Local Storms*, San Antonio, TX, Amer. Meteor. Soc., 134-137

Lakshmanan, V., 2003: Motion estimator based on hierarchical clusters. *Preprints, 19th International Conf. on Interactive Information and Processing Systems (IIPS) for Meteor., Oceanography, and Hydrology*, Long Beach, CA, Amer. Meteor. Soc., (CD Preprint).

Lakshmanan, V., K. Hondl, G. Stumpf, and T. Smith, 2003: Quality control of weather radar data using texture features and a neural network. *Preprints, 31st Radar Conference*, Amer. Meteo. Soc., Seattle, 522-525.

Lynn, R. J., and V. Lakshman, 2002: Virtual radar volumes: creation, algorithm access, and visualization. *Preprints, 21st Conf. on Severe Local Storms*, San Antonio, TX, Amer. Meteor. Soc., 229-232.

Marzban, C., and A. Witt, 2001: A Bayesian Neural Network for Severe-Hail Size Prediction. *Wea. Forecasting*, **16**, 600–610.

Mitchell, E. D., S. V. Vasiloff, G. J. Stumpf, M. D. Eilts, A. Witt, J. T. Johnson, and K. W. Thomas, 1998: The National Severe Storms Laboratory Tornado Detection Algorithm. *Wea. Forecasting*, **13**, 352-366.

Smith, T. M., K. E. Elmore, and S. A. Myers-Dulin, 2003: An improved Damaging Downburst Prediction and Detection Algorithm for the WSR-88D. *Wea. Forecasting* (submitted).

Smith, T. M., K. E. Elmore, G. J. Stumpf, and V. Lakshmanan, 2003: Detection of rotation and boundaries using two-dimensional local, linear least-squares estimates of velocity derivatives. *Preprints, 31st Conf. on Radar Meteor.*, Amer. Meteo. Soc., Seattle, 310-313.

Stumpf, G. J., A. Witt, E. D. Mitchell, P. L. Spencer, J. T. Johnson, M. D. Eilts, K. W. Thomas, and D. W. Burgess, 1998: The National Severe Storms Laboratory mesocyclone detection algorithm for the WSR-88D . *Wea. Forecasting*, **13**, 304-326.

Stumpf, Gregory J., T. M. Smith, and A. E. Gerard, 2002: The Multiple-Radar Severe Storms Analysis Program (MR-SSAP) for WDSS-II. *Preprints, 21st Conference on Severe Local Storms*, San Antonio, TX, Amer. Meteor. Soc., 138-141.

Witt, A., M. D. Eilts, G. J. Stumpf, J. T. Johnson, E. D. Mitchell, and K. W. Thomas, 1998: An enhanced hail detection algorithm for the WSR-88D. *Wea. Forecasting*, **13**, 286-303.

Zhang, J., J. J. Gourley, K. Howard, and R. A. Maddox, 2001: Three-dimensional gridding and mosaic of reflectivities from multiple WSR-88D radars. *Preprints, 30th Intl. Conf. On Radar Meteor.*, Amer. Meteor. Soc., Munich, Germany, 719-721.

Zhang, J., K. Howard, W. Xia, and J.J. Gourley, 2003: Comparison of Objective Analysis Schemes for the WSR-88D Radar Data. *Preprints, 31st Conf. on Radar Meteor.,* Amer. Meteor. Soc., Seattle, Washington, 901-910.